Electronic excitations in alkali-metal overlayers. II. Effects of substitutional adsorption of Na/Al(001)

H. Ishida
College of Humanities and Sciences, Nihon University, Sakura-josui, Tokyo 156, Japan

A. Liebsch
Institut für Festkörperforschung, Forschungszentrum Jülich, 52425 Jülich, Germany

(Received 4 November 1997)

The collective excitations in the $c(2\times2)$ Na overlayers on Al(001) are investigated by a dynamical linear-response calculation within the time-dependent local-density approximation. The Na adlayer and a few outermost Al layers are described fully three dimensionally using norm-conserving pseudopotentials while the interior of the metal is treated as semi-infinite jellium with an electron density of Al. The excitation spectrum in the low-temperature phase (hollow-site adsorption) exhibits a single broad plasmon peak, which is a mixture of the Na multipole surface plasmon and the bulklike Na overlayer plasmon. In striking contrast, the Na plasmon peak disappears completely from the spectrum in the room-temperature phase (substitutional adsorption). These observations are in good agreement with recent experiments. It is predicted that the Al vacancies in the room-temperature phase induce a large change in the excitation spectrum of the Al substrate. [S0163-1829(98)10619-7]

I. INTRODUCTION

In the past several years, major interest in the study of alkali metal chemisorption was focused on its novel structural properties. Experiments with higher accuracy revealed that alkali metal atoms adsorb not only on hollow sites but also on on-top sites.[1–3] Moreover, on a few substrates, they mix with substrate atoms and form two-dimensional (2D) surface alloys. For example, Na and K atoms on Al(001) form two different $c(2\times2)$ structures at coverage $\Theta=1/2$ (Θ is measured relative to the number of atoms in one substrate layer):[4–6] The adatoms sit on hollow sites on the unreconstructed Al layer at low temperatures (LT) while they remove every second Al atom in the first Al layer and slip into the vacancy sites at room temperatures (RT). A similar phase transition from on-top-site to substitutional adsorption was observed for the $(\sqrt{3}\times\sqrt{3})R30°$ overlayers of alkali metals on Al(111) at $\Theta=1/3$.[7,8] The formation of various super structures involving alloying of alkali metal and substrate atoms was reported also on noble metal substrates.[9,10]

When no alloying occurs, the orbital overlap between nearby adatoms is increased with increasing coverage, leading to a formation of the metallic adatom-adatom bonds with a concomitant weakening of the adatom-substrate bonding. At monolayer coverages, 2D free-electron-like resonant bands are formed in the overlayer and the overlayer exhibits quasi 2D metallic properties. In many combinations of metal substrates and alkali-metal adsorbates, collective excitations localized in the overlayer were observed at high coverages. On the other hand, in the case of substitutional adsorption, the chemical interaction between the alkali metal and substrate atoms should be appreciably enhanced due to higher coordination, which may reduce the 2D metallicity of the overlayer.

Heskett *et al.*[11] performed a core-level photoemission experiment for the LT and RT phases of K on Al(001) and Al(111) surfaces. They found that the satellite peak due to K collective modes in the LT phase disappears nearly completely in the RT phase. The disappearance of overlayer collective modes in the substitutional geometry, or at least, a drastic reduction in their intensity, was confirmed by electron energy-loss spectroscopy (EELS) by Kondoh and Nozoe[12] for K/Al(111), and very recently, by photoyield measurements by Barmen, Horn, and Häberle[13] for Na and K on Al(111). The phase transition from the LT to RT phase was also detected using second-harmonic light emission by Ying, Wang, and Plummer.[14] So far theoretical studies on this subject have been limited to the ground-state electronic structure. Apart from a number of total-energy calculations focused on structural optimizations,[15,16] two semi-infinite calculations, i.e., a Layer Korringa-Kohn-Rostoken (LKKR) Green-function calculation using muffin-tin potentials[17] and a self-consistent Green-function calculation using nonlocal pseudopotentials,[18] were performed for the Al(111) substrate. Both demonstrated that the alkali metal valence *s* resonance is strongly broadened in the case of substitutional adsorption. At present, the theoretical understanding of the difference in the nature of electronic excitations between the LT and RT phases is completely missing.

In the present work, we investigate the electronic excitations of the Na/Al(001) surface by a linear response calculation within the time-dependent local-density approximation (TDLDA).[19] For simplicity, the interior of the substrate is treated as jellium with the electron density of Al. Yet, the first few layers of the substrate Al and the Na overlayer are described fully three-dimensionally using norm-conserving pseudopotentials. Thus, both the LT and RT adsorption geometries can realistically be described by the present model. We calculate the linear response of the surface to a uniform ac electric field oriented normal to the surface as a function of frequency ω. The centroid of the induced surface charge,

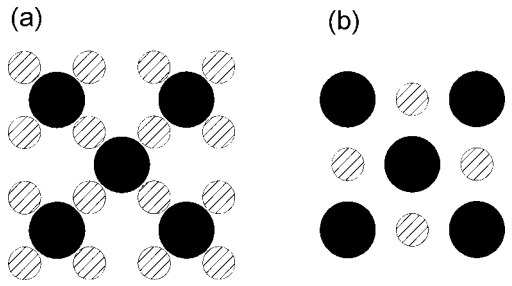

FIG. 1. Top view of the Na/Al(001) surface at $\Theta = 1/2$. The larger and smaller circles indicate Na and Al atoms, respectively.

$d_\perp(\omega)$, one of the fundamental surface response functions introduced by Feibelman,[20] is relevant to a number of surface spectroscopic experiments. Its imaginary part gives the main contribution to the surface excitation spectra in the long-wavelength limit.

Previously, we studied the electronic excitation of the Na and K overlayers on semi-infinite jellium as a function of adatom coverage.[21] As may be expected, the excitation spectrum in the LT phase where Na atoms adsorb on hollow sites of the top Al layer is similar to our previous result for Na/jellium at the full monolayer coverage. Im $d_\perp(\omega)$ exhibits one relatively broad peak centered at $\hbar\omega \sim 5$ eV, which is assigned to a mixture of the Na multipole surface plasmon and the bulklike Na overlayer plasmon. At one monolayer, the interference between these modes and their decay into electron-hole pairs is very pronounced. These peaks are clearly separated only for two or more adsorbed layers.[21,22] In striking contrast, the calculated excitation spectrum for the substitutional geometry has no noticeable peak in the energy range of Na excitations. Hence, the present results fully support the recent experimental observations mentioned above. At the same time, the transition from the LT to RT phase is found to modify the spectral shape of Im $d_\perp(\omega)$ in a wide energy range up to the bulk plasma frequency of Al. It will be shown that this change is caused by the vacancies in the first Al layer.

The plan of the present paper is as follows. In Sec. II, we describe the chemisorption model of Na on Al(001) and the outline of the computational procedure for calculating its dynamical response properties within the TDLDA. Section III is the main part of the present paper and contains results and discussion of the numerical calculations. A summary is given in Sec. IV. Unless otherwise stated, we use the Hartree atomic units throughout this paper.

II. METHOD

We consider Na adlayers on Al(001) at $\Theta = 1/2$, corresponding roughly to saturation coverage. The adatoms form a square lattice with a lattice constant $a_x = 7.66$ a.u. As stated in the Introduction, they adsorb on hollow sites on the unreconstructed Al layer at LT, while they remove one half of the Al atoms in the top layer and occupy the substitutional sites at RT (see Fig. 1).

In our previous work on the dynamical response of 3D alkali overlayers,[21] we employed the jellium model of Lang and Kohn[23] as a metal substrate. It is known that the jellium model can reproduce collective excitations of the clean Al surfaces semiquantitatively.[24] However, it can neither describe the local bonding configuration between Al and Na atoms nor the substrate reconstruction in the RT phase. In the present work, we treat not only the Na overlayer but also the outermost N_s Al layers fully three dimensionally ($N_s = 1$ to 3). On the other hand, the inner Al layers are modeled by jellium with the electron density of Al. Hereafter, we use the notation Na/Al(N_s)/jellium to denote the system. Regarding the structural parameters, we use those determined by the recent low-energy electron diffraction experiment of Berndt *et al.*[6] The nearest-neighbor (NN) Na-Al bond length is 6.18 a.u. and 5.80 a.u. for the LT and RT phases, respectively. Correspondingly, the vertical separation between the Na and top Al layers is reduced from 4.85 a.u. to 2.08 a.u. The rumpling of the third Al layer in the RT phase is incorporated in the calculation for $N_s = 3$.

The calculation consists of two major steps. First, the self-consistent Green-function calculation is performed in the embedded surface region to determine the ground-state electronic structure. In doing so, the effects of the semi-infinite substrate and vacuum are expressed via the complex embedding potential of Inglesfield.[25] A plane-wave-like basis set is utilized to expand the Green function in the embedded region, and the ion cores of Na and Al are represented by norm-conserving pseudopotentials in the Kleinman-Bylander form.[26] As for Na, the partial core correction to the exchange-correlation potential is incorporated.[27] In the actual calculation, the thickness of the embedded region is chosen as 30 a.u. It contains the vacuum region, one Na layer, N_s Al layers, and a jellium slab. The thickness of the jellium slab in the embedded region is 4 a.u. for $N_s = 3$ and 11.48 a.u. for $N_s = 1$. The distance between the edge of the positive charge background of jellium and the bottom Al layer is chosen as half the layer spacing between the adjacent Al(001) planes in the bulk, 1.915 a.u.

In the second step, we calculate the dynamical response of the surface to an external electric field with frequency ω oriented in the surface normal direction within the TDLDA. In solving the response equation for the induced density, it is essential to treat asymptotic behaviors of the induced field in the bulk metal correctly.[24] For this purpose, the Green function obtained in the embedded region is analytically extended to the whole space, and the one-electron wave functions of the semi-infinite system are derived from the Green function. Finally, the response equation is written in matrix form using a plane-wave-like basis set. As its solution we obtain the self-consistent induced charge density $n_1(\mathbf{r},\omega)$ and the screened potential. More details of the numerical procedure are described in Ref. 21.

The spectral function $d_\perp(\omega)$ introduced by Feibelman[20] is defined as the centroid of the induced charge, i.e.,

$$d_\perp(\omega) = \int d\mathbf{r}\, z n_1(\mathbf{r},\omega) \Big/ \int d\mathbf{r}\, n_1(\mathbf{r},\omega), \qquad (1)$$

where the z axis is chosen as the surface normal pointing toward the vacuum. As discussed in Ref. 21 and our preceding paper,[28] Im $d_\perp(\omega)$ is proportional to the transition rate for creating electronic excitations with energy $\hbar\omega$ in the system.

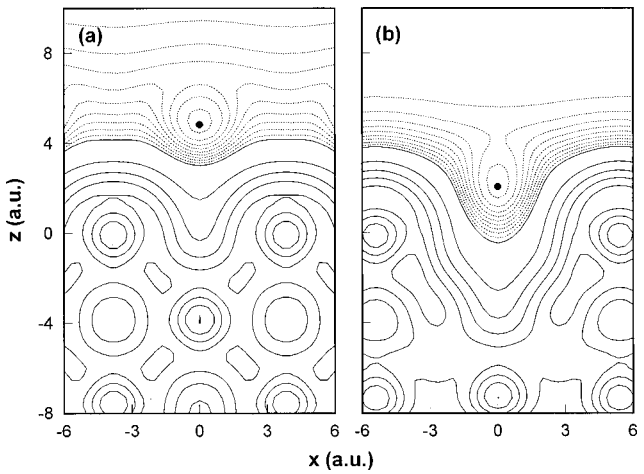

FIG. 2. Contour maps of the valence charge density for Na/Al($N_s=3$)/jellium on a vertical cut-plane containing the Na atoms and the nearest-neighbor Al atoms in the top Al layer. (a) LT phase and (b) RT phase. Contour spacing is 0.005 a.u. for solid contours and 0.0005 a.u. for dashed contours. Solid circles indicate positions of Na atoms. The z coordinate is measured relative to the top Al layer.

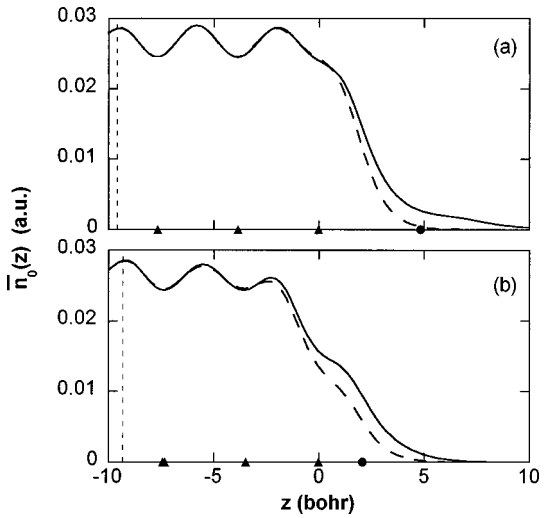

FIG. 3. Planar average of the valence charge density for Na/Al($N_s=3$)/jellium. (a) LT phase and (b) RT phase. The solid circle and triangles indicate the positions of Na and Al layers, respectively. Vertical dashed lines show the edge of semi-infinite jellium. The dashed curve in each panel shows the charge density of the substrate Al($N_s=3$)/jellium.

III. RESULTS AND DISCUSSION

A. Ground state

Figure 2 shows contour maps of the calculated valence charge density of Na/Al($N_s=3$)/jellium for the (a) LT and (b) RT phases on a vertical cut plane containing Na atoms and their NN Al atoms in the top Al layer. The solid contours with a larger spacing 5×10^{-3} a.u. characterize the charge distribution in the substrate Al, whereas dashed contours with a smaller spacing 5×10^{-4} a.u. on the vacuum side are intended for representing charge densities in the Na overlayer. The outermost solid contours in the RT phase are strongly curved toward the interior of the metal at the Al vacancy, and the Na moves into the cavity left behind. The buildup of the Al charge between the NN Na atoms in the RT phase hinders the direct interaction between them via orbital overlap. Although the charge densities in the LT and RT phases look very different, the calculated values of the work function of the two systems, 2.96 eV (LT) and 2.94 eV (RT), are almost the same.

In Fig. 3, we show the planar average of the charge density corresponding to Fig. 2. Also shown by dashed lines is the planar average of the charge density for Al ($N_s=3$)/jellium, i.e., the Na overlayer is removed from each substrate in the (a) LT and (b) RT phases. It is seen that the Na valence density of the LT structure roughly exhibits a plateau characteristic of the 2D free-standing overlayer on the vacuum side of the Na atoms, while the Na density of the RT structure is mainly piled up on the vacuum tail of the substrate Al charge density. This aspect can also be seen from Fig. 2; the spacing between dashed contours for the RT phase are appreciably contracted in the z direction as compared with that for the LT phase.

The large change in the electronic structure of the Na overlayer caused by the surface restructuring can be seen at best from the **k**-resolved adatom density of states,

$$\rho_a(\epsilon,\mathbf{k})=\frac{-1}{\pi}\int_R d\mathbf{r}\ \mathrm{Im}G(\epsilon+i\eta,\mathbf{k},\mathbf{r},\mathbf{r}), \tag{2}$$

where G denotes the Green function corresponding to energy ϵ and 2D wave vector $\mathbf{k}$, η is a positive infinitesimal, and the volume integration is performed in a sphere surrounding a Na atom with radius R (3 a.u.). Figure 4 shows the calculated $\rho_a(\epsilon)$ at four equally spaced $\mathbf{k}$ points between $\bar{\Gamma}=(0,0)$ and $\bar{X}=(\pi/a_x,0)$ for Na/Al($N_s=3$)/jellium. For the LT structure, a sharp Lorentzian-like Na 3s resonance appears below the Fermi energy ϵ_F at $\bar{\Gamma}$. It exhibits a quadratic upward dispersion with increasing k_x and crosses the Fermi level at approximately halfway between $\bar{\Gamma}$ and $\bar{X}$. At $\bar{X}$, the Na 3s resonance becomes nearly degenerate with the Na 3p_x resonance, which, contrary to 3s, has a downward dispersion

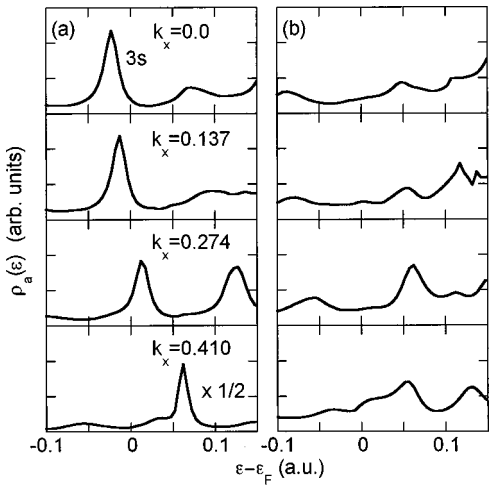

FIG. 4. **k**-resolved density of states of Na atoms for Na/Al($N_s=3$)/jellium. (a) LT structure and (b) RT structure. $R=3$ a.u. The origin of energy is the Fermi energy.

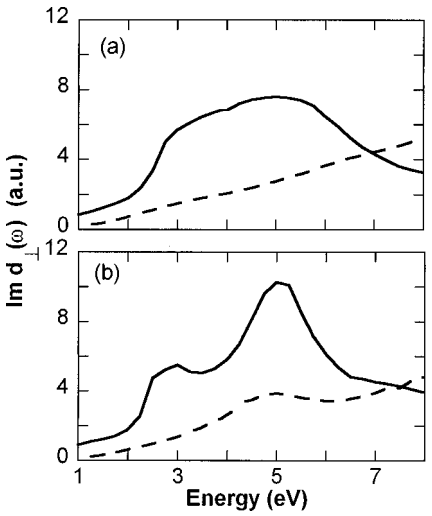

FIG. 5. Imaginary part of the spectral function $d_\perp(\omega)$ for the Na/Al(N_s)/jellium surfaces. Solid and dashed lines correspond to the LT and RT structures, respectively. (a) The number of the Al layers on semi-infinite jellium, $N_s=1$ and (b) $N_s=3$.

along the $\bar{\Gamma}$-$\bar{X}$ line. The density of states in Fig. 4(a) indicates that 2D free-electron-like resonant bands are formed in the Na overlayer. In striking contrast, the Na 3*s* resonant peak disappears almost completely from the density of states for the RT phase. The chemical interaction between the Na atom in the Al substitutional site and its four NN Al atoms is so strong that the delocalized Na 3*s* orbital component is spread over a wide energy range of the substrate Al bands. The broad peaks in Fig. 4(b) originate from the band structure of the three-layer Al slab on semi-infinite jellium and are not related to the Na valence states. A drastic broadening of the alkali metal valence *s* resonance in the substitutional structure was previously reported for the $(\sqrt{3}\times\sqrt{3})R30°$ alkali-metal overlayers on Al(111).[17,18] The present result is in line with those theoretical studies.

B. Linear response

Before discussing the results of the present numerical calculation, it is worthwhile to summarize the coverage dependence of the excitation spectra obtained in our previous work on Na overlayers on a flat semi-infinite jellium substrate.[21] At submonolayer coverages, the calculated Im $d_\perp(\omega)$ exhibited only a broad feature at around an energy corresponding to the work function. As the occupied part of the Na density of states has a broad tail-like shape, no atomiclike peak due to the Na $3s\rightarrow 3p$ transition appeared. In the monolayer regime, the threshold excitation was replaced by a broad plasmonlike peak, which was a mixture of the Na multipole surface plasmon [$\sim 0.8\hbar\omega_p$(Na)] and the bulklike Na overlayer plasmon. Finally, these two peaks grew into well-separated sharp peaks for an adsorbed double layer. The NN distance for the present Na overlayer on Al(001), $a_x=7.66$ a.u., corresponds to the monolayer range.

Now we discuss how the above-mentioned characteristic features of the overlayer excitations are modified by replacing jellium by more realistic 3D substrates. Figure 5(a) shows the calculated Im $d_\perp(\omega)$ for Na/Al($N_s=1$)/jellium. The solid and dashed lines correspond to the hollow-site (LT) and substitutional (RT) structures, respectively. For the LT phase, the calculated spectrum shows a broad peak centered at ~ 5 eV. Comparison with our previous result[21] suggests that this broad peak should be identified with a mixture of the Na multipole surface plasmon and the bulklike Na plasmon. A prerequisite for this plasmon peak is the formation of the 2D free-electron-like resonant bands in the overlayer as discussed in the preceding subsection. The calculated Im $d_\perp(\omega)$ for the RT phase is surprisingly different from that of the LT phase. It also differs considerably from Im $d_\perp(\omega)$ of the clean Al substrate. It increases almost linearly in the whole energy region of Fig. 5. As will be shown later, this behavior stems from the Al vacancies in the first Al layer.

Here we examine the dependence of the results on the number of Al layers, N_s. In Fig. 5(b) is shown the calculated Im $d_\perp(\omega)$ for Na/Al($N_s=3$)/jellium. By comparing the panels (a) and (b), one finds that the Na overlayer plasmon peak becomes narrower for $N_s=3$. As a consequence, the structure due to the threshold excitations at $\hbar\omega\sim 3$ eV, which was buried in the lower half of the broad plasmon peak for $N_s=1$, appears as a noticeable shoulder in Im $d_\perp(\omega)$. The narrowing of the plasmon peak can be explained as follows. For $N_s=3$, the Al atoms in the top layer can interact with the polarized *p* orbitals of Al atoms in the second Al layer, whereas for $N_s=1$, the top-layer Al atoms interact only with the delocalized jellium wave functions. Thus, the chemical bonding of the first Al layer to the rest of the substrate is strengthened for $N_s=3$. On the other hand, this weakens the interaction between the Na and first Al layers and enhances the quasi-2D nature of the Na overlayer. It is interesting that even the spectrum for the RT phase exhibits a broad shoulder at $\hbar\omega\sim 5$ eV for the calculation with $N_s=3$. This is unexpected because the **k**-resolved Na density of states in Fig. 4(b) for this system shows no clear Na 3*s* resonance. In principle, one should study the convergence of $d_\perp(\omega)$ as a function of the number of the Al layers. We expect that the main Na plasmon peak would not change very much upon further increasing N_s, since the large difference between $N_s=1$ and 3 is not related with the long-range Coulomb potential but originates from the short-range chemical interaction between the first and second Al layers in the ground state. On the other hand, with increasing N_s, the spectral function may exhibit fine structures due to the interband excitations in the Al layers.

The disappearance of the plasmon peak in the RT phase implies that the quasi-2D metallic nature of the Na overlayer is mostly lost. One might say that this may be expected from the **k**-resolved Na density of states in Fig. 4 alone. We emphasize, however, that the relationship between the ground-state electronic structure and the excitation spectrum is not obvious and that the latter quantity can be obtained only by performing a linear response calculation such as the present one.

Figure 6 shows the real part of $d_\perp(\omega)$. Here the origin of the *z* axis is taken as the first Al layer, and the crosses on the vertical axis indicate positions of the Na layers for the LT and RT structures. As is expected from the Kramers-Kronig relation, Re $d_\perp(\omega)$ for the LT structure decreases rapidly and crosses the Na plane at around a frequency corresponding to the Na overlayer plasmon peak. For higher energies, the Na

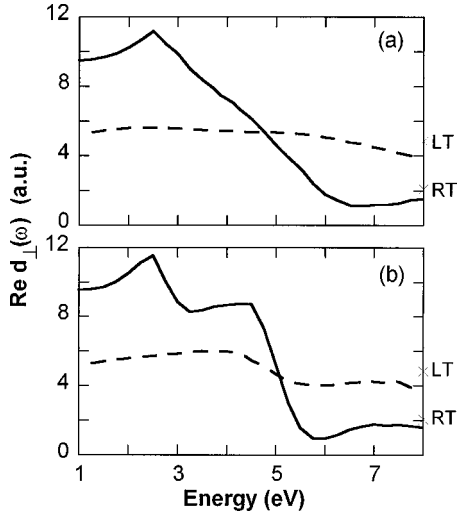

FIG. 6. Real part of the spectral function $d_\perp(\omega)$ for the Na/Al(N_s)/jellium surfaces. Solid and dashed lines correspond to the LT and RT structures, respectively. (a) The number of the Al layers on semi-infinite jellium, $N_s=1$ and (b) $N_s=3$.

overlayer becomes transparent to the applied field, and the centroid of the screening charge is located on the interface side of the Na layer. On the other hand, for the RT structure, Re $d_\perp(\omega)$ varies slowly with increasing ω. The centroid of the screening charge remains on the vacuum side of the Na layer in the whole energy range. We plotted in Fig. 7 contour maps of the real part of the normalized induced charge $n_1(\mathbf{r},\omega)/\sigma(\omega)$ for Na/Al($N_s=3$)/jellium in the LT phase for three frequencies. Since the coverage is fairly high, the screening charge distributes itself nearly one dimensionally except around the Na ion-core region where the pseudopotential is strongly repulsive. It is seen that the buildup of the positive charge density, which gives a rough estimate of Re $d_\perp(\omega)$, moves across the Na plane with increasing frequency.

Before closing this section, we discuss the influence of the vacancies in the top Al layer on the excitation spectra of the Al substrate. For this purpose, we performed an additional

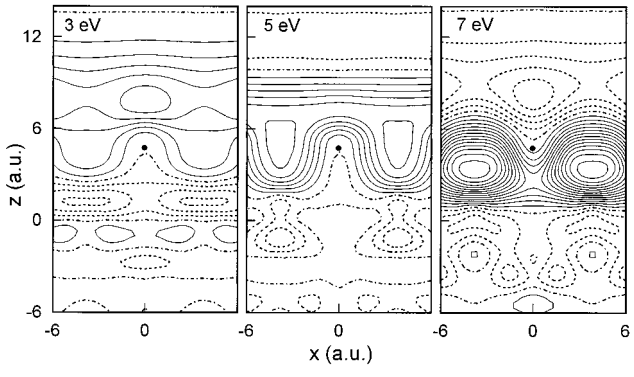

FIG. 7. Contour maps of Re $n_1(\mathbf{r},\omega)/\sigma(\omega)$ for Na/Al($N_s=3$)/jellium in the LT phase on a vertical cut-plane containing the Na atoms and the nearest-neighbor Al atoms in the top Al layer. Solid, dashed, and dot-dashed contours correspond to positive, negative, and zero values of the charge, respectively. Contour spacing is 0.05 a.u. The z coordinate is measured relative to the top Al layer.

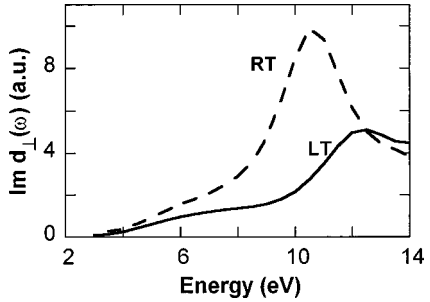

FIG. 8. Im $d_\perp(\omega)$ for the Al($N_s=1$)/jellium surfaces. Solid and dashed lines correspond to the LT and RT structures, respectively.

response calculation for the surfaces obtained by removing the Na layer from the Na/Al($N_s=1$)/jellium surfaces in the LT and RT phases. The calculated Im $d_\perp(\omega)$ for these systems are shown in Fig. 8. The surface consists of semi-infinite jellium and the 1×1 (LT) or $c(2\times2)$ (RT) Al(001) layer on top of it. The calculated spectrum for the LT structure is very similar to that of the clean jellium surface;[24] it exhibits a threshold enhancement near the energy corresponding to the work function and a broad peak due to the local-field enhancement (multipole surface plasmon) at $\sim0.8\hbar\omega_p$(Al). The former is slightly shifted to a higher energy, since the work function of the Al($N_s=1$)/jellium surface, 4.5 eV, is by ~0.6 eV larger than that of the clean jellium surface with the same electron density. For the RT structure, where every second Al atom is missing from the top Al layer, the multipole surface plasmon peak is shifted to a lower energy and its intensity is greatly enhanced, implying that the surface is more polarizable. Qualitatively, this is understandable if one assumes that the surface with vacancy atoms has an effectively lower electron density in the surface region, since it is known for clean jellium surfaces that the surface with a lower electron density is more polarizable and has a more prominent multipole surface plasmon peak.[24] This might appear surprising because the charge density in the RT phase is strongly corrugated [see Fig. 2(b)]. Thus, only the laterally averaged density is reduced. Because of the long-range nature of the Coulomb interaction, it is this average that primarily determines the mode frequencies. Similar arguments apply to the excitation spectra of low-coverage alkali-metal overlayers.[21]

The calculated Im $d_\perp(\omega)$ for the RT structure in Fig. 8 in the energy range of the Na plasmons ($\hbar\omega\leq8$ eV) is seen to be very similar to that of Na/Al(N_s)/jellium surfaces in the RT phase shown in Fig. 5. Thus, we conclude that the calculated spectral distribution in Fig. 5 for the substitutional geometry is not related to overlayer excitations. Instead, it is characteristic of the reconstructed Al substrate with a high density of Al vacancy atoms.

We have found that the excitation spectra of Na/Al(001) in the RT phase are very different from that in the LT phase not only in the energy range of the Na plasmons but also in the energy range of the Al multipole surface plasmon. The latter feature is difficult to observe with EELS because it is dominated by the monopole surface plasmon peak of Al. We hope that photoyield measurements will be performed on Na/Al(001) in a wide energy range in order to observe the enhancement of the Al multipole surface plasmon peak for the substitutional geometry. Adsorption on Al(111) might

reveal similar phenomena. However, since at most 1/3 of the Al surface atoms are displaced upon substitutional adsorption, the effects should be weaker than on Al(001).

IV. SUMMARY

We have studied the collective excitations in $c(2\times2)$ Na overlayers on an Al(001) substrate by a linear-response calculation within the TDLDA. While the interior of the metal is modeled by jellium, the Na overlayer and the outermost Al layers are treated fully three-dimensionally using nonlocal pseudopotentials. The ground-state electronic structure as well as the dynamical linear response in the long-wavelength limit are determined self-consistently using a Green-function technique based on the embedding method.

The important results obtained are as follows. The excitation spectrum in the LT phase (hollow-site adsorption) exhibits a single large peak near $\hbar\omega\sim5$ eV, which is assigned to a mixture of the Na multipole surface plasmon and the bulklike Na overlayer plasmon. In striking contrast, the Na overlayer plasmon peak vanishes nearly completely in the RT phase (substitutional-site adsorption). These observations are in good agreement with the recent core-level photoemission, EELS, and photoyield experiments. The large difference between the excitation spectra in the LT and RT structures traces back to the ground-state electronic structure: The 2D free-electron-like resonant bands formed in the Na overlayer in the LT phase are practically absent in the RT phase. It is found that the reconstructed first Al layer at RT also induces a large change in the Al-associated excitations. The Al multipole surface plasmon at RT has a much larger spectral weight than in the LT phase.

ACKNOWLEDGMENTS

One of the authors (H.I.) would like to thank the Alexander von Humboldt Stiftung for support during his one-month stay in Jülich.

[1] D. Fisher, S. Chandavarkar, I. R. Collins, R. Diehl, P. Kaukasonia, and M. Lindroos, Phys. Rev. Lett. **68**, 2786 (1992).
[2] H. Over, H. Bludau, M. Skottke-Klein, G. Ertl, W. Morotz, and C. Campbell, Phys. Rev. B **45**, 8638 (1992).
[3] D. L. Adler, I. R. Collins, X. Liang, S. J. Murray, G. S. Leatherman, K. D. Tsuei, E. E. Chaban, S. Chandavarkar, R. McGrath, R. D. Diehl, and P. H. Citrin, Phys. Rev. B **48**, 17 445 (1993).
[4] J. N. Andersen, E. Lundgren, R. Nyholm, and Q. Qvaford, Phys. Rev. B **46**, 12 784 (1992).
[5] S. Aminpirooz, A. Schmalz, N. Pangher, J. Haase, M. M. Nielsen, D. R. Batchelor, E. Bøgh, and D. A. Adams, Phys. Rev. B **46**, 15 594 (1992).
[6] W. Berndt, D. Weick, C. Stampfl, A. M. Bradshaw, and M. Scheffler, Surf. Sci. **330**, 182 (1995).
[7] A. Schmalz, S. Aminpirooz, L. Becker, J. Haase, J. Neugebauer, M. Scheffler, D. R. Batchelor, D. L. Adams, and E. Bøgh, Phys. Rev. Lett. **67**, 2163 (1991).
[8] M. M. Nielsen, J. Burchhardt, D. L. Adams, E. Lundgren, and J. N. Andersen, Phys. Rev. Lett. **72**, 3370 (1994).
[9] S. Mizuno, H. Tochihara, A. Barbieri, and A. van Hove, Phys. Rev. B **51**, 1969 (1995).
[10] S. Mizuno, H. Tochihara, A. Barbieri, and A. van Hove, Phys. Rev. B **51**, 7981 (1995).
[11] D. Heskett, E. Lundgren, R. Nyholm, and J. N. Andersen, Phys. Rev. B **52**, 12 366 (1995).
[12] H. Kondoh and H. Nozoe, Surf. Sci. **329**, 32 (1995).
[13] S. R. Barman, K. Horn, and P. Häberle (unpublished).
[14] Z. C. Ying, J. Wang, and E. W. Plummer, Surf. Sci. **363**, 289 (1996).
[15] J. Neugebauer and M. Scheffler, Phys. Rev. B **49**, 4959 (1994).
[16] C. Stampfl, J. Neugebauer, and M. Scheffler, Surf. Sci. **307-309**, 8 (1994).
[17] B. Wenzien, J. Bormet, J. Neugebauer, and M. Scheffler, Surf. Sci. **287/288**, 559 (1993).
[18] H. Ishida, Surf. Sci. **388**, 71 (1997).
[19] A. Zangwill and P. Soven, Phys. Rev. A **21**, 1561 (1980).
[20] P. J. Feibelman, Prog. Surf. Sci. **12**, 287 (1982).
[21] H. Ishida and A. Liebsch, Phys. Rev. B **45**, 6171 (1992).
[22] A. Liebsch, Phys. Rev. Lett. **67**, 2858 (1991).
[23] N. D. Lang and W. Kohn, Phys. Rev. B **1**, 4555 (1970).
[24] For a review, see A. Liebsch, *Electronic Excitations at Metal Surfaces* (Plenum, New York, 1997).
[25] J. E. Inglesfield, J. Phys. C **14**, 3795 (1981).
[26] L. Kleinman and D. M. Bylander, Phys. Rev. Lett. **48**, 1425 (1982).
[27] S. G. Louie, S. Froyen, and M. L. Cohen, Phys. Rev. B **26**, 1738 (1982).
[28] H. Ishida and A. Liebsch, preceding paper, Phys. Rev. B **57**, 12 550 (1998).